GPS Solut (2017) 21:639–650
DOI 10.1007/s10291-016-0554-9

ORIGINAL ARTICLE

Global ionosphere maps based on GNSS, satellite altimetry, radio occultation and DORIS

Peng Chen[1] · Yibin Yao[2,3] · Wanqiang Yao[1]

Received: 14 July 2015 / Accepted: 7 July 2016 / Published online: 20 July 2016

Abstract Global ionosphere maps (GIMs) provided by the global navigation satellite systems (GNSS) data are essential in ionospheric research as the source of the global vertical total electron content (VTEC). However, conventional GIMs experience lower accuracy and reliability from uneven distribution of GNSS tracking stations, especially in ocean areas with few tracking stations. The orbits of ocean altimetry satellite cover vast ocean areas and can directly provide VTEC at nadir with two different wavelengths of radio waves. Radio occultation observations and the beacons of Doppler orbitography and radio positioning integrated by satellite (DORIS) are evenly distributed globally. Satellite altimetry, radio occultation and DORIS can compensate GNSS data in ocean areas, allowing a more accurate and reliable GIMs to be formed with the integration of these observations. This study builds GIMs with temporal intervals of 2 h by the integration of GNSS, satellite altimetry, radio occultation and DORIS data. We investigate the integration method for multi-source data and used the data in May 2013 to validate the effectiveness of integration. Result shows that VTEC changes by −11.0 to −7.0 TECU after the integration of satellite altimetry, radio occultation and DORIS data. The maximum root mean square decreases by 5.5 TECU, and the accuracy of GIMs in ocean areas improves significantly.

Keywords Global ionosphere maps · Total electron content · GNSS · Satellite altimetry · Radio occultation · DORIS

Introduction

The ionosphere is an important part of the earth's upper atmosphere, approximately located between 60 and 1000 km above the surface of the earth where the plasma affects the propagation of electromagnetic waves. Ionospheric delay of electromagnetic wave is related to signal frequency, which is utilized to detect and model the ionosphere (Yuan 2002). Among the ionospheric models, observational models are commonly employed and are built by modeling ionosphere observations with mathematical methods (Mannucci et al. 1998). Each ionospheric data analysis center of International GNSS Service (IGS) provides GIMs with the temporal interval of 2 h and daily differential code bias (DCB) of satellites and receivers (Feltens 2003; Hernández-Pajares et al. 2009).

Early GIMs were developed using only global positioning system (GPS) data and further in combination of global navigation satellite system (GLONASS). However, GNSS tracking stations are only located on land, which results in limited accuracy and reliability of GIMs in ocean areas. Thus, different spatial and temporal distributions as well as different observation characteristics and sensitivities concerning ionospheric parameter estimation from various techniques can be integrated to make full use of their advantages (Dettmering et al. 2011).

✉ Peng Chen
chenpeng0123@gmail.com

[1] College of Geomatics, Xi'an University of Science and Technology, Xi'an 710054, China

[2] School of Geodesy and Geomatics, Wuhan University, Wuhan 430079, China

[3] Key Laboratory of Geospace Environment and Geodesy, Ministry of Education, Wuhan University, Wuhan 430079, China

Research has been conducted on establishment of the global ionospheric model using multi-source data. Todorova et al. (2007) created GIMs from GNSS and satellite altimetry observations. Results showed that a higher accuracy of the combined GIMs over the ocean areas was achieved based on the advantages of each particular type of data with higher accuracy and reliability. However, the precise weights of these two types of observations were not determined. Dettmering et al. (2011) computed regional models of VTEC based on the IRI 2007 and observations from ground GNSS stations, radio occultation data from low earth orbiters, dual-frequency radar altimetry measurements and data obtained from Very Long Baseline Interferometry. Alizadeh et al. (2011) investigated global modeling of the total electron content through combining GNSS and satellite altimetry data with global TEC data derived from the occultation measurements of COSMIC. The combined GIMs of VTEC show a maximum difference of 1.3–1.7 TECU compared with the GNSS-only GIMs in a day. The root mean square (RMS) maps of the combined solution show a reduction of about 0.1 TECU over a day, but not in combination with the observations of Doppler orbitography and radio positioning integrated by satellite (DORIS) and VTEC, and no precise weight of different observations was obtained. Chen and Chen (2014) introduced a new global ionospheric modeling software—IonoGim, using ground-based GNSS data, altimetry satellite and LEO (Low Earth Orbit) occultation data to establish the global ionospheric model. GIMs and DCBs obtained from IonoGim were compared with the CODE (Center for Orbit Determination in Europe) to verify its accuracy and reliability. In addition, through comparison between using only ground-based GNSS observations and multi-source data model, it can be demonstrated that the space-based ionospheric data effectively improve the model precision in marine areas. Chen et al. (2015) used both ground-based GNSS data and space-based data from ocean altimetry satellite and radio occultation to establish a global ionospheric model, the bias between the space-based ionospheric data and ground-based GNSS data were seen as parameters to estimate. The results showed that, by adding space-based data, the accuracy of GIMs over the ocean areas improves to make up the deficiencies of the existing GIMs.

DORIS is designed for precise orbit determination and is effective for ionospheric research (Auriol and Tourain 2010). Thus, integrating DORIS data can further improve the accuracy of GIMs over the ocean areas.

This study includes satellite altimetry, radio occultation and DORIS data in the global ionospheric modeling process and investigates the integration approach of global ionospheric modeling with multi-source data. The results are compared with models using GNSS-only, and the effectiveness of multi-source data integration is analyzed. This study also considers the bias between different systems and uses variance component estimation to determine the refined weights of different observations.

Acquisition of ionospheric VTEC

When the signals pass through the ionosphere, they will be delayed by amounts that are inversely proportional to the square of the signal frequency. Using dual-frequency signals, one can obtain information about the ionosphere, i.e., VTEC. Systems such as GNSS, ocean altimetry satellite, ionospheric occultation and DORIS can obtain ionospheric VTEC. This section provides a brief introduction.

Acquisition of ionospheric VTEC from GNSS

The Slant Total Electron Content (STEC) can be calculated from double-frequency GNSS observations as shown in the equation (Schaer 1999; Yuan 2002):

$$\mathrm{STEC} = \frac{f_1^2 f_2^2}{40.3(f_1^2 - f_2^2)}(P_2 - P_1 + \Delta b_k + \Delta b^s) \quad (1)$$

where P_1 and P_2 are code observations of the two frequencies, f_1 and f_2 are frequencies, and Δb_k and Δb^s are receiver and satellite DCBs. In practical modeling, the method of phase-smoothing the pseudorange is commonly employed to diminish noise of code observations. The maximum error in the STEC calculation process is DCB (Li et al. 2012), which is usually considered a daily constant and estimated as a parameter together with ionospheric model coefficients by least squares.

When modeling the global ionospheric map, it is often assumed that all electrons in the ionosphere are concentrated in a thin shell at altitude H, which is usually presumed 350–500 km. We assume a height of 450 km. The intersection of the signal path and this thin shell is called ionospheric pierce point. TEC along the signal path (STEC) can be projected into VTEC using the trigonometric functions, namely,

$$\mathrm{STEC} = mf \cdot \mathrm{VTEC} \quad (2)$$

where $mf = 1/\sqrt{1 - \left(\frac{R}{R+H}\sin z\right)^2}$, R is the earth radius, H is the altitude of the ionospheric thin shell, and z is the zenith distance at receiver's location.

Acquisition of VTEC from satellite altimetry

Ocean altimetry satellites mainly include TOPEX/Poseidon and its follow-on missions Jason-1 and Jason-2. These satellites have a 1336 km circular, non-sun-synchronous orbit with an inclination of 66° with respect to the earth's

equator. The altimeter on board has two frequencies including the main Ku band (13.575 GHz) and assistant C band (5.3 GHz). Let dR can be calculated as presented by Brunini et al. (2005) without the need of a mapping function, we obtain,

$$\mathrm{VTEC} = -\frac{dR \cdot f_{\mathrm{Ku}}^2}{40.3} \tag{3}$$

The value dR can be directly obtained from the differential group path of the signal by means of altimetry, and f_{Ku} is the Ku-band carrier frequency. VTEC data from altimetry satellite are a valuable resource for evaluating the accuracy of GIM TEC maps, especially for the ocean altimetry applications, with an accuracy of 2–3 TECU (Imel 1994).

Acquisition of VTEC from radio occultation

GPS radio occultation measurements on Low Earth Orbit (LEO) satellites have some advantages compared with terrestrial GPS data, e.g., they are globally distributed and are not limited to continental regions (Fong et al. 2009).

The radio occultation technique has high accuracy, high vertical resolution and global coverage. The Constellation Observation System of Meteorology, Ionosphere and Climate (COSMIC) is the main occultation system currently operational, providing about 2000 global occultation events everyday. VTEC below the satellites is directly provided by the University Corporation for Atmospheric Research (UCAR) through its product "ionPrf". The position of the maximal electron density is used as the location for the profile. Dettmering et al. (2011) and Alizadeh et al. (2011) also used the same data as we used.

Acquisition of VTEC from DORIS

DORIS is a French Doppler satellite tracking system developed for precise orbit determination and precise ground positioning. In order to eliminate ionospheric delay in the propagation of signals from ground beacons to satellites, DORIS adopts a double-frequency observing scheme. The two frequencies are $f_1 = 2036.25$ MHz and $f_2 = 401.25$ MHz.

The new generation DORIS receiver DGXX, first installed in Jason-2, is capable of transmitting not only similar Doppler data as the last two generations, but also data in form of RINEX having double-frequency code and phase observations. Phase observations from DORIS have millimeter accuracy and are highly applicable for ionospheric modeling.

The preprocessing method of RINEX 3.0 data from DORIS is similar with GPS due to the similarity in data form. Mercier et al. (2010) conducted research on processing of DORIS double-frequency phase observation data. The accuracy of the code observations is 1–5 km (Mercier et al. 2010). In this study, we only adopt the high-precise phase observations to model ionospheric TEC and solve related ambiguities. The DORIS double-frequency phase observation equations are:

$$\begin{aligned}
\lambda_1\varphi_1 &= D_1 + c(\tau_r - \tau_e) - \frac{40.3 \cdot \mathrm{STEC}}{f_1^2} + V_{\mathrm{tro}} - \lambda_1 N_1 + \varepsilon_1 \\
\lambda_2\varphi_2 &= D_2 + c(\tau_r - \tau_e) - \gamma\frac{40.3 \cdot \mathrm{STEC}}{f_1^2} + V_{\mathrm{tro}} - \lambda_2 N_2 + \varepsilon_2
\end{aligned} \tag{4}$$

where λ_1 and λ_2 are wavelengths of L_1 and L_2 signals transmitted from ground beacons, φ_1 and φ_2 are phase observations of the two frequencies, $\gamma = f_1^2/f_2^2$, V_{tro} is tropospheric delay, N_1 and N_2 are ambiguities of L_1 and L_2, ε_1 and ε_2 are observational noises, τ_r and τ_e are time errors of receiving and transmitting, respectively. Differencing (4) yields,

$$\begin{aligned}
\mathrm{STEC} = \frac{f_1^2 f_2^2}{40.3\left(f_1^2 - f_2^2\right)}[&(\lambda_1\varphi_1 - \lambda_2\varphi_2) \\
&-(\lambda_1 N_1 - \lambda_2 N_2) - (\varepsilon_1 - \varepsilon_2)]
\end{aligned} \tag{5}$$

Ignoring the influence of $\varepsilon_1 - \varepsilon_2$, the biased TEC without ambiguity can be calculated as below:

$$\mathrm{STEC}_{\mathrm{bias}} = \frac{f_1^2 f_2^2 (\lambda_1\varphi_1 - \lambda_2\varphi_2)}{40.3\left(f_1^2 - f_2^2\right)} \tag{6}$$

Then, an external ionospheric model such as IRI and GIMs is used to correct $\mathrm{STEC}_{\mathrm{bias}}$ and obtain STEC without bias.

Despite its high accuracy, the DORIS STEC obtained using phase observation does not consider the impact of integer ambiguity, and there is a constant bias between the actual STEC and DORIS STEC. As a result, the DORIS STEC is only a relative STEC and cannot be directly used for modeling. In this study, $\mathrm{STEC}_{\mathrm{bias}}$ is corrected by using GIMs model as mentioned above. First, the initial GIMs are built using GNSS-only data. The VTEC at IPPs of DORIS observations is calculated from initial GIMs and projected onto the signal propagation path. Then, the difference between the STEC from GIMs and STEC directly calculated from DORIS in each successive observational arc (with no cycle slip occurring) is employed to get the average bias. Next, each DORIS STEC is corrected by adding the average bias in corresponding successive observation arc and projected onto zenith direction to obtain a revised VTEC. Eventually, DORIS VTEC is corrected once again using GIMs with the addition of DORIS data in order to obtain more accurate DORIS VTEC. The DORIS VTEC correction process is shown in Fig. 1.

The corrected DORIS VTEC is used in global ionospheric modeling together with VTEC obtained by GNSS,

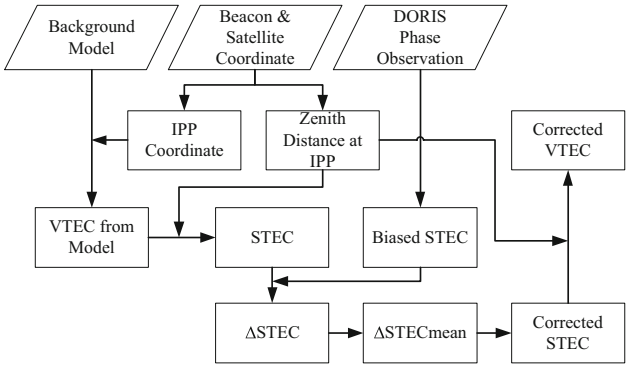

Fig. 1 DORIS VTEC correction flowchart

satellite altimetry and radio occultation. Variance component estimation is used to determine the refined weights of all kinds of observations.

Combination strategy

The observations described in the previous section are combined in a single joint VTEC model. The Center for Orbit Determination in Europe applies the commonly used spherical harmonic function with a degree and order of 15 to build GIMs. The spherical harmonic function can be expressed as (Schaer 1999; Yuan 2002):

$$\mathrm{VTEC}(\beta,s)=\sum_{n=0}^{N}\sum_{m=0}^{n}\tilde{P}_{nm}(\sin\beta)(\tilde{C}_{nm}\cos(\mathrm{ms})+\tilde{S}_{nm}\sin(\mathrm{ms})) \tag{7}$$

where β is the geocentric latitude of the ionospheric pierce point, $s=\lambda-\lambda_0$ is the sun-fixed longitude of the ionospheric pierce point, λ is the longitude of the ionospheric pierce point, λ_0 is the longitude of the sun, N is the maximum degree of the SH expansion, $\tilde{P}_{nm}(\sin\beta)$ is the normalized associated Legendre function of degree n and order m, $\tilde{C}_{nm}$ and $\tilde{S}_{nm}$ are the unknown coefficients of the spherical harmonic functions, i.e., the global ionosphere model parameters.

We also take the degree and order of 15 spherical harmonic function; the temporal resolution of the model is 2 h, and treat the bias of VTEC between satellite altimetry, DORIS and GNSS as constants over 2 h, treat the bias of VTEC between radio occultation and GNSS as daily constants, and estimate them together with spherical harmonic coefficients. The DCBs for all GNSS satellites and receivers are computed daily as constant values, with a zero-mean condition imposed on the DCBs of the satellites.

The parameters to be estimated include spherical harmonic coefficients of 256 model parameters in each epoch, DCBs of GNSS satellites and receivers, and bias of satellite altimetry, radio occultation and DORIS with respect to GNSS. The normal equation matrix is:

$$\begin{aligned} N_{\mathrm{comb}} &= N_{\mathrm{GNSS}}+N_{\mathrm{ALT}}+N_{\mathrm{RO}}+N_{\mathrm{DORIS}} \\ &= B_{\mathrm{GNSS}}^{T}P_{\mathrm{GNSS}}B_{\mathrm{GNSS}}+B_{\mathrm{ALT}}^{T}P_{\mathrm{ALT}}B_{\mathrm{ALT}} \\ &\quad +B_{\mathrm{RO}}^{T}P_{\mathrm{RO}}B_{\mathrm{RO}}+B_{\mathrm{DORIS}}^{T}P_{\mathrm{DORIS}}B_{\mathrm{DORIS}} \end{aligned} \tag{8}$$

where N is the normal equation matrix, B is the design matrix, P is the weight matrix. In order to save computer space and improve computing speed, the method of normal equations stacking is adopted, and only nonzero elements are considered.

Due to different accuracies of different observations, the Helmert variance component estimation (VCE) is used to estimate variance factors of each data source priori to obtain reasonable weights of different kinds of observations. Then, the equations can be solved by least-squares adjustment. The Helmert variance component estimation can be expressed as shown in Koch and Kusche (2002) and Chen et al. (2015). During the modeling process, the iterative method is used to remove observations whose error is greater than 3 times of mean square error.

Then, the final GIMs and error maps are derived using spherical harmonic coefficients and corresponding estimation error. The estimation error σ can be computed by (Schaer 1999; Zhang and Tang 2014):

$$\sigma=ef\cdot\hat{\sigma}_0\cdot\sqrt{q} \tag{9}$$

where $\hat{\sigma}_0$ is the estimated variance of unit weight, q is the VTEC cofactor calculated by the cofactors of spherical harmonic coefficients according to the cofactor propagation law, and ef is the error factor which is set to 10 according to the processing method in CODE.

Observation data

This study uses data of May 2013 (day of year: DoY 121–151) to validate the effectiveness of using multi-source data integration to improve the accuracy and reliability of GIMs in ocean areas.

The GNSS data have a temporal interval of 30 s and a cutoff elevation angle of 15°. The DORIS data have a temporal interval of 10 s and a cutoff elevation angle of 10°. The original temporal interval of Jason-1/-2 data is 1 s. We choose medians of raw data in 180 s for sliding average and resample data with a temporal interval of 10 s.

GNSS data

The global distribution of 233 IGS GNSS stations used in this study is shown in Fig. 2. Among them, 144 stations contain observations of both GPS and GLONASS. Though

the number of stations increases globally, the distribution of the IGS global tracking stations is still very uneven. There are large gaps in the south-central Pacific Ocean, south of the Atlantic Ocean, south of the Indian Ocean, the Sahara Desert in North Africa and Antarctica.

Satellite Altimetry data

Ionospheric data provided by satellite altimetry cover the ocean area. Footprints of Jason-1/-2 in DoY 121, 2013 are shown in Fig. 3. The VTEC from Jason-1/-2 mainly covers oceans in 66°S–66°N, allowing the replenishment of the ionospheric observations.

COSMIC radio occultation data

The COSMIC radio occultation data distribution is shown in Fig. 4. There are a total of 1051 COSMIC ionospheric occultation events in DoY 121, 2013. COSMIC radio occultation events are evenly distributed in both the ocean and the land areas between ±75°. Adding the VTEC obtained by COSMIC radio occultation is helpful to improve the accuracy and reliability in the ocean areas.

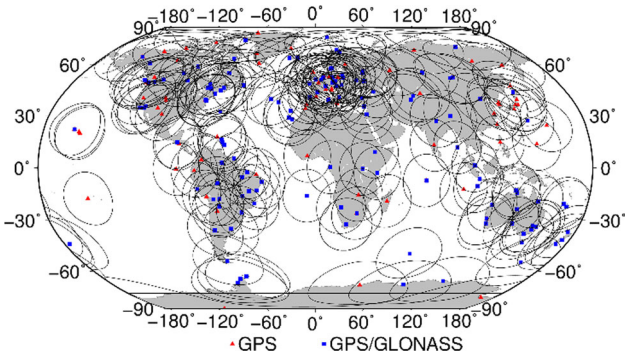

Fig. 2 Global distribution of 233 IGS GNSS stations in DoY 121, 2013. *Triangles* indicate locations of GPS stations, *squares* indicate locations of GPS/GLONASS stations, and *black circle* indicates the probed ionospheric regions

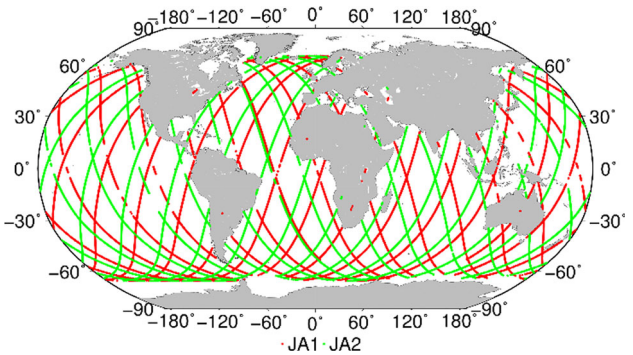

Fig. 3 Distribution of VTEC data of DoY 121, 2013 from Jason-1/-2

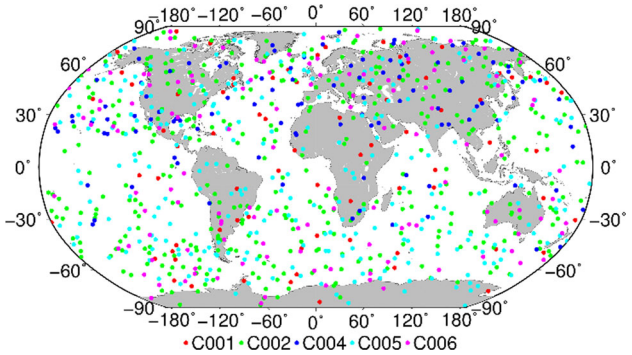

Fig. 4 Distribution of VTEC data from COSMIC, DoY 121, 2013

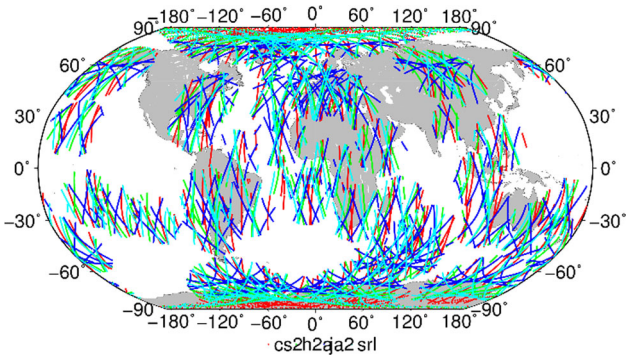

Fig. 5 Global distribution of DORIS footprints for DoY 121, 2013

DORIS data

Figure 5 depicts the footprints of four DORIS satellites in DoY 121, 2013. The footprints are distributed densely in the ocean areas, especially in the southeast of the Pacific Ocean, south of the Atlantic Ocean, south of the Indian Ocean and the Antarctic areas with limited GNSS stations. As a result, the accuracy of the GIMs is expected to increase by including DORIS observations into the integration procedure.

Results and comparison

This section compares the GIMs using only ground GNSS observations and those with GNSS and satellite altimetry data, GNSS and radio occultation observations, GNSS and DORIS observations, as well as GNSS, satellite altimetry, radio occultation and DORIS, respectively. The impact on GIMs after adding satellite altimetry, radio occultation and DORIS observations is then analyzed.

GIMs from GNSS

The final GIMs and error maps at 10:00 UT of DoY 121, 2013, calculated using GNSS-only data, are shown in Fig. 6. The global distribution and variation of ionospheric VTEC is represented well, and the ionospheric equatorial anomaly is clearly shown. The estimation error in most areas is low, but is significantly large in several regions with sparsely distributed GNSS stations, indicating that the model accuracy is related with data distribution density. Accuracies are higher over the land areas, while lower in the ocean areas, especially in the north and southeast of the Pacific Ocean, south of the Atlantic Ocean and south of the Indian Ocean near the South Pole. The estimation error in these areas even reaches 8.5 TECU. Therefore, if GNSS-only data are used to build GIMs, the uneven distribution of stations may lead to lower accuracy and reliability in ocean areas. The bottom panel shows the global distribution map of GNSS ionospheric pierce point between 09:00 and 11:00 UT. Large gaps of IPPs exist in ocean and the other areas, and the lack of observational data in these areas directly leads to the significantly higher estimation error than other regions in middle panel.

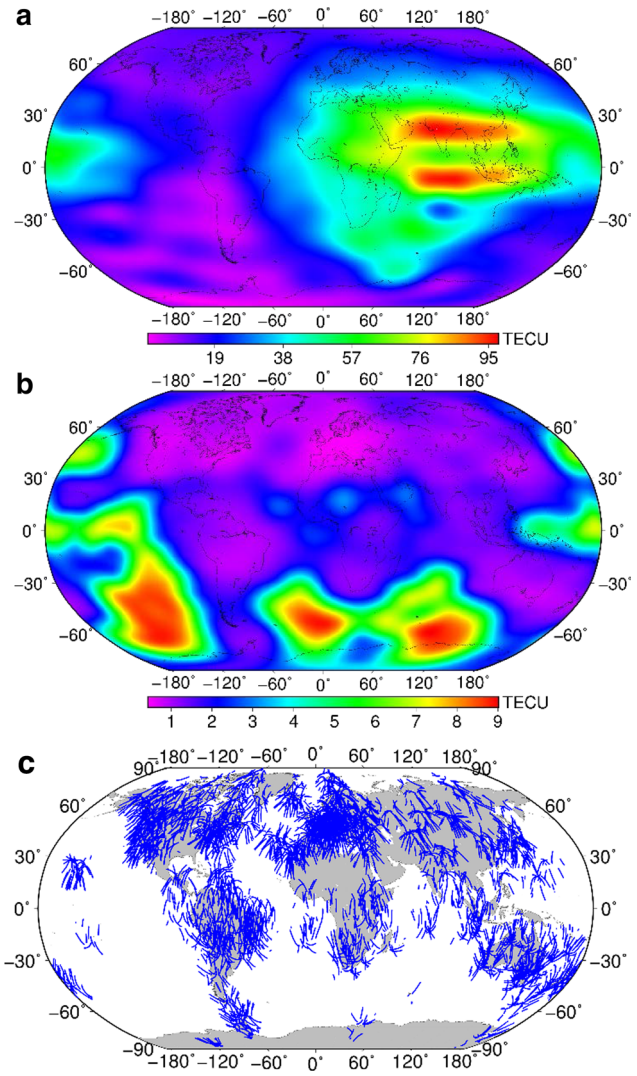

Fig. 6 Final GIMs (*top*) and error maps (*middle*) at 10:00 UT of DoY 121, 2013 modeled by GNSS data and IPP global distribution between 09:00 and 11:00 UT (*bottom*)

GIMs from GNSS and satellite altimetry

Figure 7 shows that VTEC changes greatly in the ocean areas. VTEC decreases by about 11 TECU at (180°E, 0°N) and its vicinity, increases by 4 TECU in the South Pacific

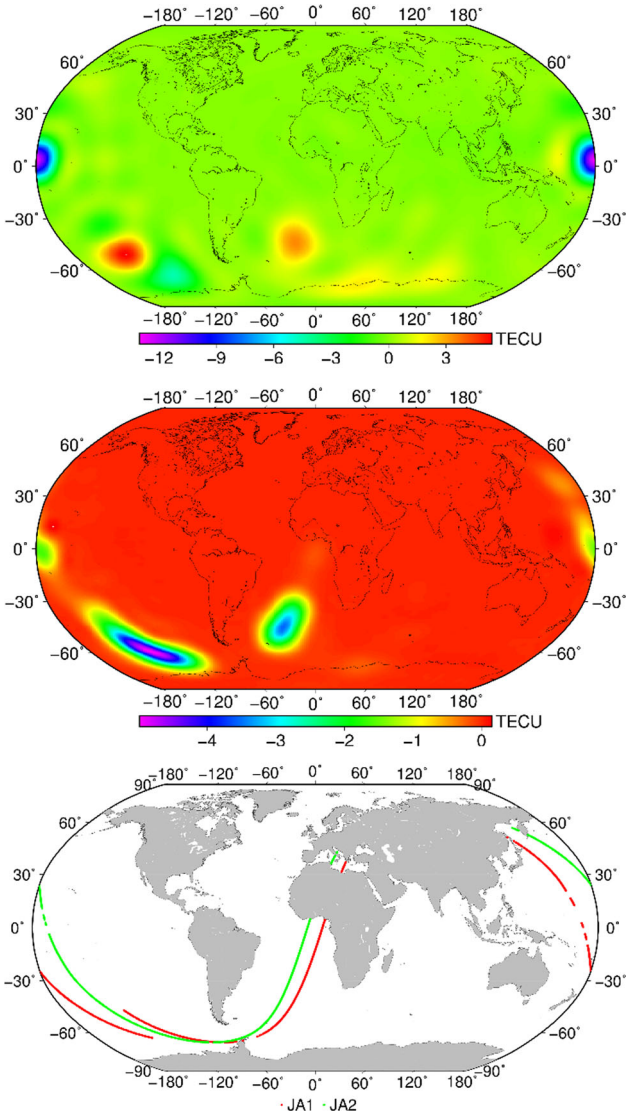

Fig. 7 Differences of VTEC (*top*) and estimation error (*middle*) at 10:00 UT of DoY 121, 2013 between those modeled with GNSS-only data and those modeled with both GNSS and altimetry data, and the footprints of satellite altimetry between 09:00 and 11:00 UT in DoY 121, 2013 obtained from Jason-1/-2 (*bottom*)

region, and increases by 3 TECU in the South Atlantic region. After adding satellite altimetry data, the overall estimation error decreases, while increases in some low accuracy regions are detectable. The largest reduction reaches 5 TECU at (180°E, 0°N) and its vicinity. The estimation error reduces 2–3 TECU in south of the Atlantic Ocean. The differences of VTEC and estimation error shown in Fig. 7 indicate that the accuracy in ocean areas is improved by combining satellite altimetry data. The improvement of accuracy coincides with the footprints of satellite altimetry. The area with the reduction of the estimation error is exactly the region with satellite altimetry data coverage, and the area with the most significant estimation error declination is exactly the region with most densely distributed satellite altimetry data.

GIMs from GNSS and radio occultation

This section provides the differences between the GIMs using only GNSS data and GIMs by integration of GNSS data and radio occultation data. The comparison results of VTEC and estimation error are illustrated in Fig. 8. As shown, the VTEC changes (−0.3 to −0.45 TECU) after adding radio occultation data are much smaller than the changes after adding ocean altimetry data. The most significant VTEC changes occur mainly in the ocean areas in the southern hemisphere. For example, the VTEC increases by 0.4 TECU in the South Pacific near 30°S due to the small number and discrete distribution of COSMIC observations with little effect on final results. The area with the most significant VTEC and estimation error change corresponds to the area with denser radio occultation data distribution and lower number of ground GNSS tracking stations.

GIMs from GNSS and DORIS

The differences between VTEC and estimation error calculated with GNSS-only data and with both GNSS and DORIS data at 10:00 UT of DoY 121, 2013 are demonstrated in Fig. 9. VTEC changes between −6.0 and 3.0 TECU by adding DORIS data. Accuracies of GIMs, especially in the southeast of the Pacific and the Antarctic areas, are improved significantly with a decrease of over 5 TECU, while insignificant changes are shown on land, reflecting subtle effect on areas with dense GNSS observations. Although the distribution of DORIS data in Europe, South America and the Atlantic region is more dense, the VTEC and estimation error changes are very small, because the distribution of ground GNSS tracking stations and DORIS observations is sparser in the regions. Most IPPs in the 2 h are located at the ocean areas and the Antarctic. The accuracies of GIMs modeled with GNSS and DORIS data are significantly improved in the ocean areas, while little or no

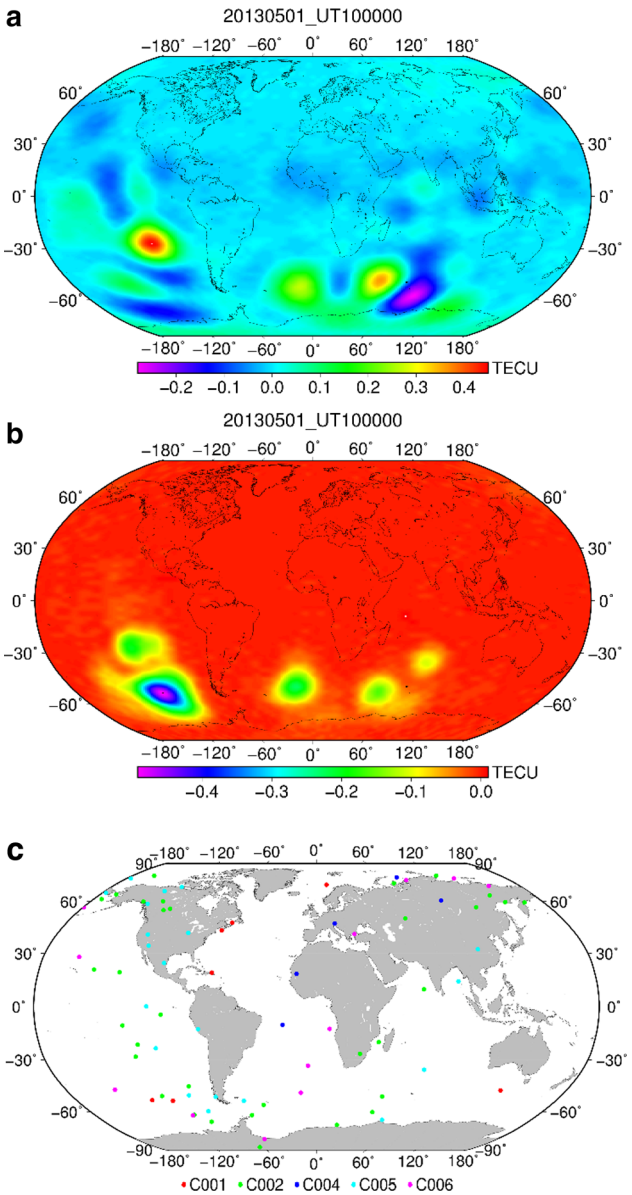

Fig. 8 Differences of VTEC (*top*) and estimation error (*middle*) at 10:00 UT of DoY 121, 2013 between those modeled with GNSS-only data and those modeled with both GNSS and radio occultation, and global COSMIC radio occultation distribution during 09:00–11:00 UT (*bottom*)

improvement can be detected on land in comparison with GIMs modeled with GNSS-only data.

GIMs from GNSS, satellite altimetry, radio occultation and DORIS

According to the analysis above, adding satellite altimetry, radio occultation and DORIS data into the combination procedure will presumably offer globally denser distribution for the observations, especially in the ocean areas. Integrating multi-source data can make use of their

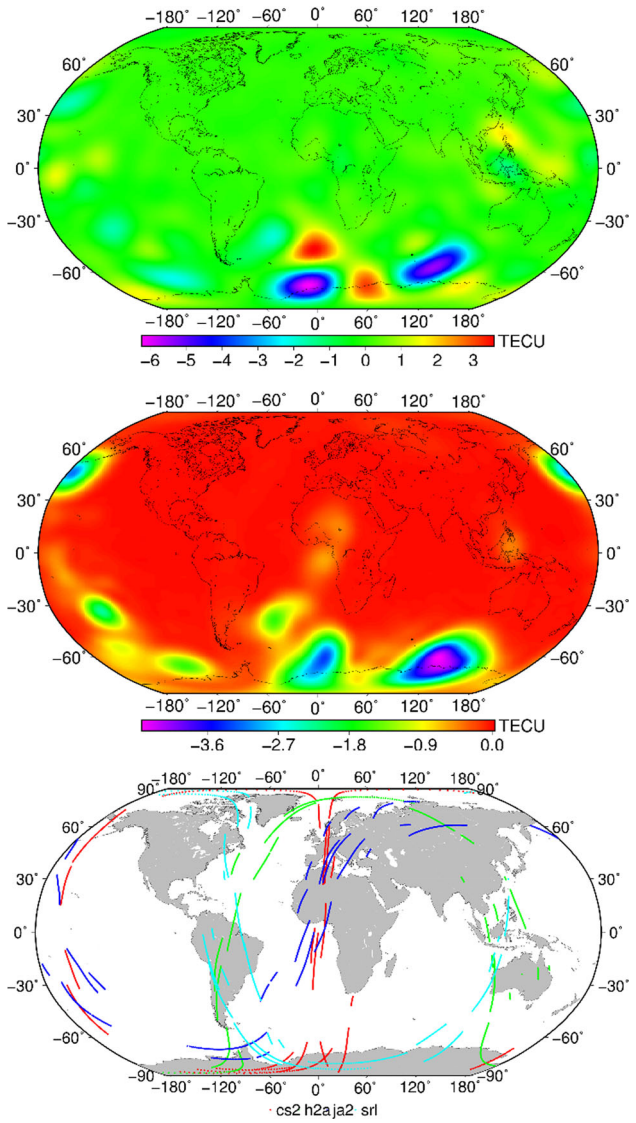

Fig. 9 Differences of VTEC (*top*) and estimation error (*middle*) at 10:00 UT of DoY 121, 2013 between those modeled with GNSS-only data and those modeled with both GNSS and DORIS data, the global distribution of IPPs of DORIS rays in 09:00–11:00 UT of DoY 121, 2013 (*bottom*)

advantages and achieve more accurate GIMs. Figure 10 shows the differences of VTEC and estimation error between models only with GNSS data and models developed using combination of multi-source data. VTEC changes significantly from −11.0 to 5.0 TECU after multi-source data integration, and the accuracy of GIMs is improved significantly with a decrease of 5.5 TECU. Comparison among Figs. 7, 8, 9 and 10 indicates that areas with improved accuracies are largest when modeling GIMs by the integration of GNSS, satellite altimetry, radio occultation and DORIS. This result indicates that combining data from more kinds of technique may help achieving higher accuracy in larger areas.

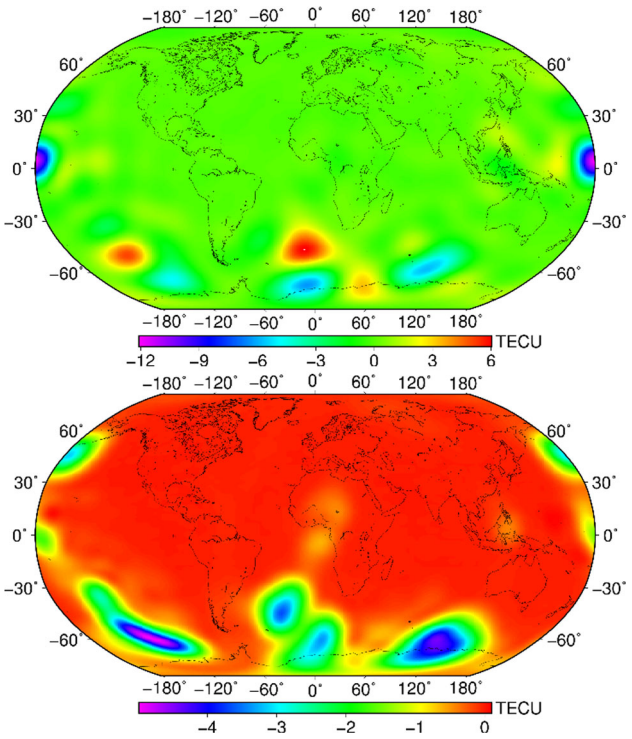

Fig. 10 Differences of VTEC (*top*) and estimation error (*bottom*) at 10:00 UT of DoY 121, 2013 between those modeled with GNSS-only data and those modeled with integration of GNSS, satellite altimetry, radio occultation and DORIS

Validation and analysis

Ocean altimetry and COSMIC radio occultation observations that are not involved in the modeling process are used in this section to validate the accuracy of all results. The weights and systematic error of various kinds of observations are also analyzed.

External accuracy test

The mean absolute error (MAE) is chosen as criterion to evaluate the models. The expressions of MAE is,

$$\mathrm{MAE} = \frac{1}{N}\sum_{i=1}^{N} \left| y_i' - y_i \right| \tag{10}$$

where y_i' and y_i are modelled values and observed values, respectively, and N is the number of observations.

The VTEC obtained by Jason-1/-2 and COSMIC satellites is treated as true value, and the modeled VTEC at the same position is obtained by interpolating from GIMs. Then, the difference between the two (considering the bias of satellite altimetry and COSMIC) is calculated. Finally, MAE can be obtained by (10).

Validation with Jason-1/-2

Parts of the observations from Jason-1/-2 not involved in modeling are used as the true value to validate the model. The MAE of the two GIMs in each day is also calculated as shown in Fig. 11. The GIMs using multi-source data with Jason-1/-2 VTEC are better than that using only ground GNSS data. The average for MAE of GIMs using multi-source data with Jason-1/-2 within 31 days in May 2013 is 2.88 TECU and 2.90 TECU, respectively, and is 0.47 TECU (14.02 %) and 0.44 TECU (13.17 %) less than the monthly average using only GNSS data. A smaller difference between GIMs using multi-source data and Jason-1/-2 original observations indicates that the accuracy of GIMs using multi-source data in ocean regions is improved.

Validation with COSMIC

To further validate the accuracy of GIMs using multi-source data, we use part of observations from five COSMIC satellites which are not involved in modeling as the true value and calculate the MAE of the two GIMs in each day. Figure 12 shows the difference between the MAE of GIMs using multi-source data and those using only ground GNSS data within 31 days. Most MAE differences are less than zero, indicating that the GIMs using multi-source data are closer to COSMIC original observations. The monthly average of MAE of multi-source data is 0.09 TECU lower than that of GNSS only.

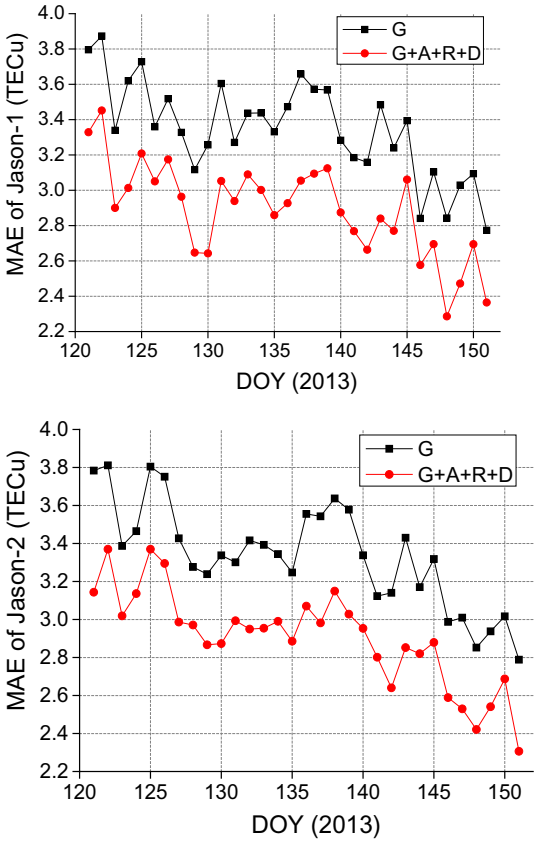

Fig. 11 Distribution of MAE of GIMs using GNSS data and GIMs using multi-source data in DoY 121–151, 2013

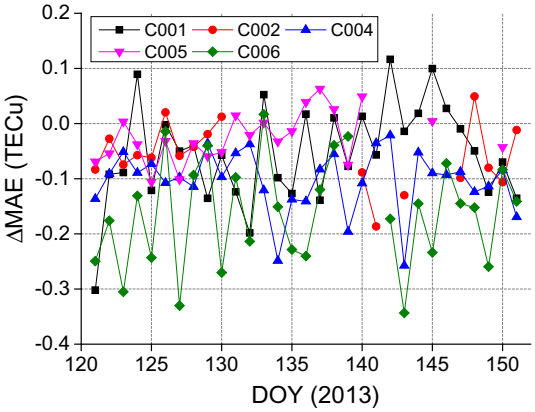

Fig. 12 Differences between MAE of multi-source data and MAE of ground GNSS data in DoY 121–151, 2013

Analysis of weights

In this study, when determining the precise weight of different kinds of observations using variance components estimation, we treat the weight of GPS observations as a constant that equals 1 and further determine the weights of other observation techniques.

The statistical result of the weight of various observations in 31 days is shown in Table 1. The weight of GLONASS is lowest, with the average of only 0.37 and standard deviation of 0.03. Weights of Jason-1/-2 and five COSMIC satellites are all close to 0.5, while the accuracy

Table 1 Statistics of weights of various observation in DoY 121–151, 2013. The weight of GPS is regarded as a constant and equal to 1

	Max	Min	Mean	SD
GLONASS	0.41	0.31	0.37	0.03
JA1	0.66	0.39	0.48	0.07
JA2	0.63	0.38	0.48	0.06
C001	0.76	0.27	0.46	0.11
C002	0.58	0.32	0.43	0.07
C004	0.79	0.37	0.51	0.10
C005	0.51	0.33	0.40	0.05
C006	0.69	0.33	0.44	0.09
Cryosat-2	1.17	0.66	0.87	0.13
HY-2A	1.13	0.61	0.86	0.14
Jason-2	1.59	0.84	1.11	0.20
Saral	1.48	0.73	1.07	0.17

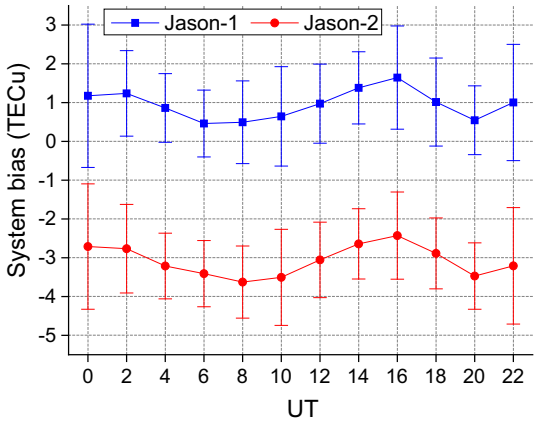

Fig. 13 Monthly average of bias between the satellite altimetry VTEC and GPS systems in DoY 121–151, 2013

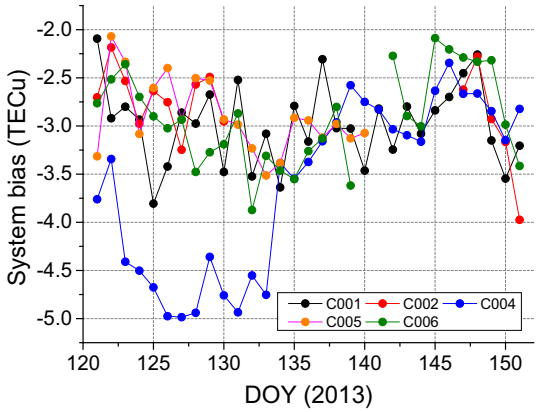

Fig. 14 Bias between the VTEC obtained by COSMIC satellites and GPS systems in DoY 121–151, 2013

of VTEC obtained by DORIS is highest. The average weight of Cryosat-2 and HY-2A is close to 0.9, while the weight of Jason-2 and Saral is larger than 1.

Analysis of bias

The bias of various techniques with respect to GNSS is calculated in this section. The bias of every COSMIC satellite in 1 day is treated as a constant. The bias of Jason-1/-2 and DORIS satellite is treated as a constant within 2 h. The monthly average and standard deviation of the bias at every 2 h of each satellite are calculated.

The monthly average and standard deviation of systemic bias of Jason-1/-2 satellite in every 2 h are shown in Fig. 13. The monthly averages of bias of Jason-1 and Jason-2 have a similar trend, with the maximum in 16:00 UT and the minimum in 06:00–08:00 UT. The average of Jason-1 is about 0.95 TECU and that of Jason-2 is −3.08 TECU, showing that the average VTEC obtained by Jason-1 is 0.95 TECU larger than the GPS VTEC, while the VTEC obtained by Jason-2 is 3.08 TECU smaller than the GPS VTEC.

The bias of 5 COSMIC satellites relative to the GPS VTEC in DoY 121–151, 2013 is illustrated Fig. 14. The bias of C001, C002, C005 and C006 changes slightly within 31 days. The monthly averages are, respectively, −2.99, −2.80, −2.90 and −2.92 TECU, indicating that VTEC obtained by COSMIC is on average about 2.9 TECU smaller than GPS VTEC. The bias of C004 during DoY 123–133 is significantly lower than on other days, with an average of −4.71 TECU. But in the remaining days, the bias of C004 is consistent with other satellites.

The monthly average and standard deviation of bias of corrected DORIS VTEC are shown in Fig. 15. The biases of the four satellites are oscillating around zero. The mean biases of Cryosat-2, HY-2A, Jason-2 and Saral are, respectively, −0.03, −0.01, −0.10 and 0.12 TECU, indicating that there is no significant bias between GPS VTEC and the corrected DORIS VTEC.

Conclusions

In this study, the GIM models are established by integration of multi-source data such as GNSS, satellite altimetry, radio occultation and DORIS data. The biases between different data are considered and are estimated together with ionospheric model parameters. The bias of each ocean altimetry satellite and each DORIS satellite is treated as a constant over 2 h, and the bias of each radio occultation satellite in 1 day is also treated as a constant. According to the accuracy differences of ionospheric data from different systems, the Helmert variance component estimation is used to obtain the weights of different types of observations.

The effect on the accuracy of GIMs by integrating satellite altimetry, radio occultation and DORIS data is analyzed using observations on DoY 121–151, 2013. The result shows that the estimation error decreases by 5.5 TECU after adding satellite altimetry, radio occultation and DORIS data, and the accuracy of GIMs is improved significantly in the ocean areas.

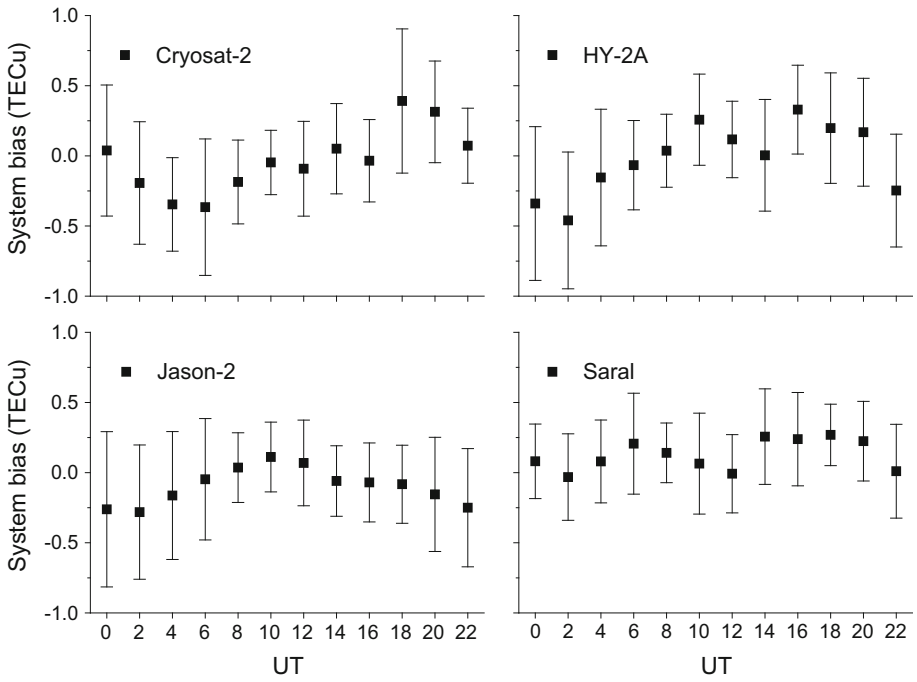

Fig. 15 Monthly average of systematic differences between the DORIS VTEC and GPS systems in DoY 121–151, 2013

Since more and more satellites can offer ionospheric observations and the accuracy of the ionospheric observations improves, multi-source ionospheric integration has great potential to create higher-accuracy GIMs, especially in the ocean areas where ground GNSS stations are inadequate.

Acknowledgments We thank CDDIS for providing GNSS and DORIS observation data, CNES and NOAA for providing Jason-1 and Jason-2 GDR data, respectively, NOAA for providing ionosonde data and CDAAC for providing COSMIC "ionprf" data. This study was funded by the National Natural Science Foundation of China (41404031) and Key Laboratory of Geo-informatics of State Bureau of Surveying and Mapping (201420).

References

Alizadeh M, Schuh H, Todorova S, Schmidt M (2011) Global ionosphere maps of VTEC from GNSS, satellite altimetry, and Formosat-3/COSMIC data. J Geodesy 85(12):975–987

Auriol A, Tourain C (2010) DORIS system: the new age. Adv Space Res 46(12):1484–1496

Brunini C, Meza A, Bosch W (2005) Temporal and spatial variability of the bias between TOPEX- and GPS-derived total electron content. J Geod 79(4–5):175–188

Chen P, Chen J (2014) The multi-source data fusion global ionospheric modeling software—IonoGim. Adv Space Res 53(11):1610–1622

Chen P, Yao W, Zhu X (2015) Combination of ground-and space-based data to establish a global ionospheric grid model. IEEE Trans Geosci Remote Sens 53(2):1073–1081

Dettmering D, Schmidt M, Heinkelmann R, Seitz M (2011) Combination of different space-geodetic observations for regional ionosphere modeling. J Geod 85(12):989–998

Feltens J (2003) The international GPS service (IGS) Ionosphere working group. Adv Space Res 31(3):635–644

Fong C-J, Yen NL, Chu C-H, Yang S-K, Shiau W-T, Huang C-Y, Chi S, Chen S-S, LiouY-A KuoY-H (2009) FORMOSAT-3/COSMIC spacecraft constellation system, mission results, and prospect for follow-on mission. Terr Atmos Ocean Sci 20:1–19

Hernández-Pajares M, Juan JM, Sanz J, Orus R, Garcia-Rigo A, Feltens J, Krankowski A (2009) The IGS VTEC maps: a reliable source of ionospheric information since 1998. J Geodesy 83(3–4):263–275

Koch KR, Kusche J (2002) Regularization of geopotential determination from satellite data by variance components. J Geodesy 76(5):259–268

Li Z, Yuan Y, Li H, Ou J, Huo X (2012) Two-step method for the determination of the differential code biases of COMPASS satellites. J Geodesy 86(11):1059–1076

Mannucci AJ, Wilson BD, Yuan DN, Ho CH, Lindqwister UJ, Runge TF (1998) A global mapping technique for GPS-derived ionospheric total electron content measurements. Radio Sci 33(3):565–582

Mercier F, Cerri L, Berthias JP (2010) Jason-2 DORIS phase measurement processing. Adv Space Res 45(12):1441–1454

Schaer S (1999) Mapping and predicting the earth's ionosphere using the Global Positioning System. Ph.D. thesis, Bern University, Switzerland

Todorova S, Schuh H, Hobiger T (2007) Using the global navigation satellite systems and satellite altimetry for combined global ionosphere maps. Adv Space Res 42:727–736

Yuan YB (2002) Theory and method research of GPS-based ionospheric monitoring and delay correction. Institute of Geodesy and Geophysics, CAS, Wuhan

Zhang X, Tang L (2014) Daily global plasmaspheric maps derived from cosmic GPS observations. IEEE Trans Geosci Remote Sens 52(10):6040–6046

Peng Chen received the Ph.D. degree in geodesy and surveying engineering from Wuhan University, Wuhan, China, in 2012. He is currently a Lecturer with the College of Geomatics, Xi'an University of Science and Technology, Xi'an, China. His main research interests include global ionospheric modeling using multisource geodesy observations, 3-D ionospheric tomography and ionospheric anomaly analysis under abnormal conditions.

Yibin Yao received the B.Sc., Master's, and Ph.D. degrees in geodesy and surveying engineering from Wuhan University, Wuhan, China, in 1997, 2000 and 2004, respectively. He is currently a Professor with Wuhan University. His main research interests include global navigation satellite system ionospheric/atmospheric/meteorological studies, theory and method of surveying data processing, and GPS/MET and high precision GPS data processing.

Wanqiang Yao received the Ph.D. degree from Chang'an University, Xi'an, in 2004. He is currently the Dean and a Professor with the College of Geomatics, Xi'an University of Science and Technology, Xi'an. His research interests include 3S integration and applications, and remote sensing and geographical conditions monitoring.